J. Earth Syst. Sci. (2022)131 105
https://doi.org/10.1007/s12040-022-01840-1

Origin of silicic breccio-conglomerate within the ~2.5 Ga LIP rhyolites, Bastar craton (India) and its volcanological and stratigraphic implications

Sarajit Sensarma* and Ruchi Gaur

Department of Geology, University of Lucknow, Lucknow 226 007, India.
**Corresponding author. e-mail: sensarma2009@gmail.com*

MS received 23 May 2021; revised 18 September 2021; accepted 2 December 2021

Recognition of ancient pyroclastic rocks made up of particles of explosive volcanic origin and deposited by primary volcanic processes and/or rapid sedimentation of freshly erupted, texturally unmodified particles *vis-a-vis* secondary volcaniclastic deposits derived by significant reworking during transport of primary volcanic particles prior to deposition, but long after volcanism (epiclastic) remains a major challenge. A volcanic conglomerate having both rhyolitic clasts and matrix within the ~2.5 Ga Bijli Rhyolite in the Dongargarh large igneous province in the Bastar craton, is earlier interpreted to be of epiclastic origin, primarily because of the presence of large rounded rhyolite clasts imparting conglomeratic appearance to the deposit, and thereby considered representing a significant time break (unconformity) between explosive Bijli volcanism and the deposit. Based on new field and petrography studies, we identified the ~125 m thick volcanic conglomerate as rapidly sedimented texturally unmodified rhyolitic breccia-conglomerate linked to coeval incipiently welded pyroclastic flow that occurred during caldera collapse related to mafic-recharge-mediated Bijli volcanism, without significant time break. We ascribed the rounding of rhyolite clasts to surface tension of hot crystallising molten magma in plastic state and partly to mechanical interactions of particles on steep slopes in such volcanic settings. This study may help clarify origin of similar deposits in deformed metamorphosed provinces elsewhere.

Keywords. Pyroclastic; rhyolite; large igneous province; Palaeoproterozoic; Dongargarh; India.

1. Introduction

There has been a tremendous interest in the study of silicic rocks in large igneous provinces (LIPs) in recent times (e.g., Bryan *et al.* 2010; Shellnutt *et al.* 2012; Sharkove *et al.* 2017; Troll *et al.* 2019). Since the recognition of bimodal LIP (Sensarma 2007 and references therein) having subequal proportions of silicic and mafic rocks, accumulations of synchronous silicic to high silicic volcanic rocks seem ubiquitous even in mafic LIPs (e.g., Bryan *et al.* 2010 and references therein; Rooney *et al.* 2010; Ghose *et al.* 2016; Cheng *et al.* 2017; Sensarma *et al.* 2018; Halder *et al.* 2021).

Diverse physical processes operate during LIP emplacement (White *et al.* 2009). However, field and petrographic criteria for recognition and characterisation of silicic primary pyroclastic deposits, resedimented pyroclasts and epiclastic

This article is part of the Topical Collection: Deccan Traps and other Flood Basalt Provinces – Recent Research Trends.
Published online: 22 April 2022

volcanic particles/volcaniclastic deposits, though remain a major challenge, are key to interpret their processes-based origins (e.g., Ross and Smith 1961; Fisher 1966; Fiske 1969; Wright *et al.* 1980; Cas and Wright 1987; Fisher and Smith 1991; McPhie *et al.* 1993 and references therein; Müller *et al.* 2000; de Silva 2008; Sensarma *et al.* 2017; Gooday *et al.* 2018). Recently, Sohn and Sohn (2019) used the term 'reprocessed' for syn-eruptive volcaniclastic fragments, deposited finally by non-volcanic processes (secondary deposit), irrespective of the exact reworking processes involved. The problem of recognition of Precambrian silicic volcanic deposits gets further complicated because the rocks are subjected to deformation and metamorphism, erosion and other secondary processes leading sometimes to equivocal interpretations.

Understanding the physical and volcanological processes from silicic volcaniclastic deposits in the Indian Precambrian LIPs are limited, except for some preliminary studies in the Dalma volcanic belt in the Singhbhum craton (e.g., Gupta *et al.* 1977; Gupta and Basu 2000), the Dongargarh province (Mukhopadhyay *et al.* 2001) and the Malani rhyolites (e.g., Sharma 2004; Vallinayagam and Kumar 2007). Within the ∼2.5 Ga Bijli Rhyolite, the large silicic volcanic and volcaniclastic rocks (SiO_2 >72 wt%), in the Dongargarh LIP (Bastar craton), Sarkar (1956, 1957, 1958) identified an interesting rock type in which rounded 'pebble to cobble-sized clasts' of rhyolitic compositions are set in a fragmental to micro-fragmental matrix of similar compositions. He described the rock as rhyolitic conglomerate and ascribed an epiclastic origin as in a normal sedimentary setting for the deposit, which unconformably overlies the Bijli Rhyolite.

The aim of this paper is to characterise and reinterpret the origin of the Sarkar's rhyolite conglomerate in light of recent understanding of volcanic processes in LIPs in general and the Dongargarh LIP in particular. The paper presents (i) new field data, (ii) describe detailed thin section petrography for the deposit and then (iii) combine the results to discuss, that the 'rhyolite conglomerate' is of primary pyroclastic origin linked to caldera collapse (Bijli volcanism) as part of the Dongargarh LIP event, without any unconformable relationship among the breccio-conglomerate deposit, the Bijli rhyolites and the overlying basalts; rather recognised as a member within the Bijli Rhyolite.

2. Geological setting

The ∼2.5 Ga Dongargarh bimodal LIP in the Bastar craton (Sensarma 2005, 2007) represents a thick (8–10 km) volcanic–sedimentary succession of rocks where large volume of silicic volcanic and volcaniclastic rocks of rhyolite to high silica rhyolite (SiO_2 >75 wt%), called Bijli Rhyolite (figure 1), occurs early in the succession (Sensarma and Mukhopadhyay 2003, 2014), not commonly known in the literature. Dongargarh granite intrudes the volcanic–sedimentary succession of rocks (e.g., Ramachandra and Roy 1998). Sarkar (1957, 1958) first presented a geological map for the Dongargarh province and identified the main structure as a northerly plunging syncline (Sitagota syncline) plunging 20°N.

Occurrence of subequal proportions of near-coeval silicic and younger mafic volcanic rocks (including Fe-rich basaltic andesite), granitoids and interspersed sedimentary rocks of both mature and immature types covering >50,000 km^2 in a continental rift setting characterises the province (Sensarma 2007 and references therein). The Dongargarh rocks are metamorphosed at a low-grade green-schist facies metamorphism, and a penetrative N–S fabric parallel to the axial surface of the regional syncline is discernible in the rocks. Since the pioneering study of Sarkar (1957, 1958, 1994), although a number of geochemical studies on the Dongargarh volcanics have been carried out in recent years (e.g., Sensarma *et al.* 2002, 2004 and references therein; Sensarma and Palme 2013; Manikyamba *et al.* 2016), there has been little systematic field and texture/microstructure study on volcanic rocks, particularly on diverse silicic volcanic rocks hosted in the province.

The Bijli Rhyolite, the basal lithostratigraphic unit of the Dongargarh group (table 1), comprises silicic volcanic rocks of rhyolite to high silica rhyolite (SiO_2 ∼65–80 wt%), is as thick as 4 km at places (e.g., south to WSW of Salekasa) and >8000 km^3 in volume (Sensarma *et al.* 2004), and perhaps represents one of the most conspicuous ancient LIP rhyolite occurrences. The Bijli Rhyolite is well exposed in the western limb of the regional synclinal structure. Diverse fragmental rocks of explosive origin within Bijli Rhyolite are identified, that include high-grade rheoignimbrites, ignimbrites, welded tuff, breccias, massive and banded rhyolite related to plinian eruption (Mukhopadhyay *et al.* 2001; Sensarma *et al.* 2004). Sarkar (1956, 1957, 1994) identified different

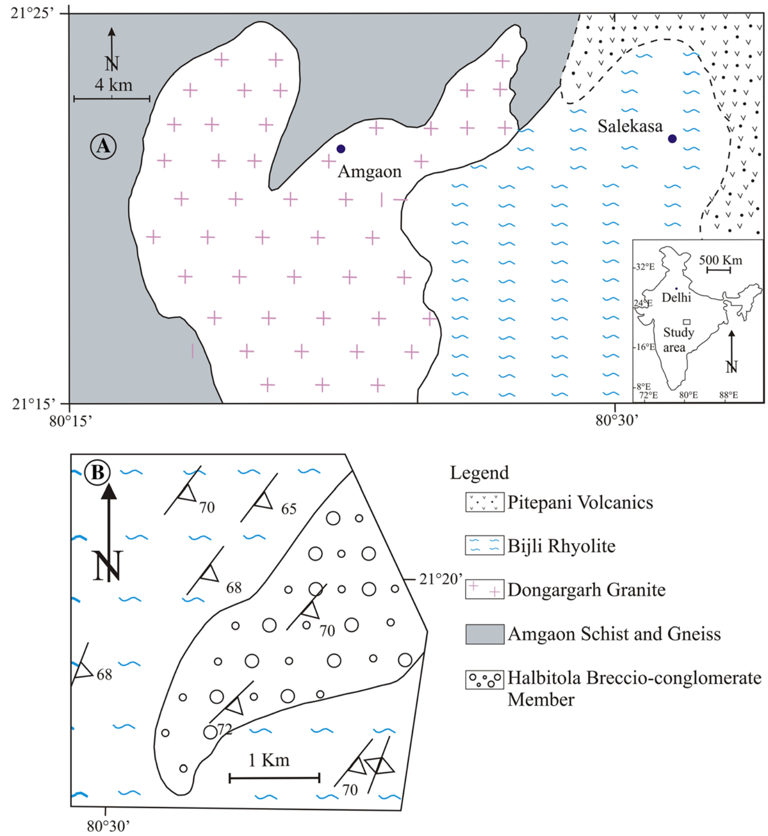

Figure 1. (**A**) Geological map (modified after Deshpande *et al.* 1990) around Amgaon–Salekasa sector in the Dongargarh LIP, on the western limb of the regional Sitagota syncline. (**B**) Silicic breccio-conglomerate (Halbitola breccio-conglomerate member) within the Bijli Rhyolite located about 3 km east to south-east of Salekasa. Map of India (inset) showing location of study area. For further details of the deposit and adjacent areas on larger scale (1:25,000), see Chakraborty and Sensarma (2008) and Sensarma and Mukhopadhyay (2014).

banded rhyolitic flow rocks within the Bijli Rhyolite. Ignimbrites and other associated rocks vary in both crystallinity and bulk compositions. The eruption temperature of the Bijli volcanism is estimated at ~900°C (Sensarma *et al.* 2004). The initial $^{87}Sr/^{86}Sr$ of the Bijli rhyolites is similar to the bulk continental crust (~0.703) at ca. 2.5 Ga (0.7057 ± 0.0015, Sarkar *et al.* 1981; 0.70305 ± 0.0017, Krishnamurthy *et al.* 1990). The low-$\delta^{18}O$ rhyolites ($\delta^{18}O$ <5‰), typical of its rarity, are present (Sensarma *et al.* 2004, 2018).

Silicic conglomerate within the Bijli Rhyolite is Bhattacharya's 'conglomerated and recrushed mylonites' (*op. cit.*, see Fermor 1934, 1935), which Sarkar (1956, 1957, 1958) later identified as rhyolitic conglomerate of epiclastic origin and assigned as 'lava conglomerate' of Pettijohn (see Sarkar 1957, 1958). In this rock, interestingly, both clasts and matrix are of rhyolitic compositions. Owing to the presence of both angular and well-rounded rhyolitic fragments, the deposit is described as breccio-conglomerate in this study.

Limited geochronological data are available on the Dongargarh rocks. Bijli Rhyolite, the basal unit of the Dongargarh group (figure 1; table 1) yielded Rb–Sr isochron ages of 2180 ± 25 Ma (Sarkar *et al.* 1981) to 2503 ± 35 Ma (Krishnamurthy *et al.* 1990). The large range of the Rb–Sr dates is probably due to disturbance of the isotopic system during deformation and metamorphism. Later, the U–Pb single-crystal zircon dating of the oldest rhyolite in the Kotri belt, the southern extension of the Dongargarh belt, has yielded an emplacement age of ~2530 Ma (Ghosh 2004). A more recent study on the $^{207}Pb/^{206}Pb$ spot ages from zircons of the Pitepani basalts and Bijli Rhyolite (see table 1) from the Kotri region in the southern part of the belt range from 2446 to 2522 Ma (weighted mean age 2471 ± 7 Ma), and 2479 ± 13 Ma and 2463 ± 14 Ma, respectively (Manikyamba *et al.* 2016). Thus, the Bijli Rhyolite and basalts are nearly coeval. Geochemical and petrogenetic linkage amongst basalts (Pitepani and Sitagota basalts) and the evolved Fe-rich andesite (Mangikhuta

Table 1. *Stratigraphic relations among rhyolites (Bijli Rhyolite), silicic breccio-conglomerate and basalts (Pitepani Volcanics) in the Dongargarh province, Central India.*

Sarkar (1957–1958, 1994)			Sensarma and Mukhopadhyay (2003, 2014)	
			Bijepar Formation (low dipping immature sediments)	
			Unconformity	
			Dongargarh Granite	
			Intrusive contact	
Dongargarh Supergroup	Khairagarh Group	Mangikhuta Volcanics	Mangikhuta Volcanics	**Dongargarh Group**
		Karutola Formation	Karutola Formation	
		Sitagota Volcanics	Sitagota Volcanics	
		Bortalao Formation	Chandsuraj Formation	
		Unconformity	Pitepani Volcanics	
	Nandgaon Group	Dongargarh Granite	Bijli Rhyolite	
		Pitepani Volcanics	(with Halbitola Rhyolitic Breccio-conglomerate Member)	
		Unconformity		
		Bijli Rhyolite	Basement?	
		Unconformity		
Amgaon Group (basement gneiss, etc.)				

andesite) (Sensarma 2007; Sensarma and Palme 2013; Sensarma and Mukhopadhyay 2014; see table 1) also establish near contemporaneity of volcanism in the province at ca. 2.5 Ga.

3. Field characters and internal architecture

This N–S to NNE–SSW trending rhyolite breccio-conglomerate rock could be traced laterally (1:25,000) for about 3 km, and is best exposed in detached outcrops east and south-east of Salekasa (21°21′:80°32′) on the western limb of the regional Sitagota synclinal structure. Due to distinct lithological characteristics and spatial distribution, it is given a status of a member within the Bijli Rhyolite, known as Halbitola breccio-conglomerate (Sensarma and Mukhopadhyay 2003, 2014). The large clasts are aligned or tend to align along the N/N10°E trending crude foliation, parallel to the axial trace of the regional 'Sitagota syncline'; foliation dips at about 60° towards east. The foliation is occasionally discernible in the matrix of the rock. Effects of deformation, low-grade green schist facies metamorphism and other secondary processes render recognition of original characteristics of the rock difficult in the field. Nevertheless, original textures/microstructures (e.g., vesicular pumice, vitroclastic textures and embayed subhedral feldspars) are reasonably better preserved in the rock.

The ∼125 m thick reasonably well exposed deposit overall is a matrix-supported oligomictic breccio-conglomerate with/without thin interspersed phyric tuff (possibly described earlier rhyolite porphyry; see Sarkar 1957, 1958). The gradual transition from breccia to conglomeratic appearance of the rock is towards stratigraphic younging direction, i.e., towards east, but without any visible mineralogical changes. The lower boundary of the deposit is not exposed in the area, though rhyolitic crystal tuff may occasionally be encountered in the vicinity of the western boundary of the deposit. The upper boundary is, however, exposed at places, that mark the contact with rhyolitic tuff ± banded rhyolite having larger crystals.

In the lower part of the section studied for nearly 25–30 m, the rock is a volcanic breccia (figure 2). Within the brecciated part, the framework clasts (30%) comprise abundant angular to subangular buff to grey-coloured rhyolite ignimbrite fragments (lithics), crystals of quartz and feldspar, often broken and vitric clasts (rhyolitic pumice) set in a dense aphanitic to micro-fragmental matrix. The rock is generally massive, though fine to very fine banding is discernible within the matrix locally parallel to the regional N–S trending fabric.

In the field, angular to subangular rhyolitic lithic fragments, crystals and some glassy (devitrified) particles set in matrix make up the framework clasts (table 2). The angular framework clasts vary in size; 2–6 cm seem more common, though clasts as large as >12 cm are also present (figure 3a and b). Dense, grey-to-dark-grey framework clasts with vague outline set within the dense aphanitic to microgranular matrix are sometimes difficult to recognise because of the lack of colour contrasts (figure 3b), attributable to compositional similarities of both these framework clasts and matrix in the rock. Angularities of the rhyolitic framework clasts in general reduce with their size, i.e., larger the fragments lesser the angularities. In fact, better rounding of larger clasts essentially imparts a conglomeratic appearance to the rock (figure 3c). The matrix of these clasts comprises smaller fragments (<5 mm). At places, matrix contains green clots/patches of chlorite.

Further up the section, within the next 10–12 m the rocks imperceptibly grade into conglomeratic appearance (figures 2 and 3c–e). Although the lack of exposures makes extent of the gradation between breccias and conglomerate zone uncertain, the smaller rhyolitic framework clasts (2–6 cm), however, still maintain angularity in the gradational zone denoting the lithological continuity.

The conglomeratic (80–90 m thick) part constitutes the major portion of the deposit, perhaps what prompted Sarkar (1957, 1958) to assign the rock 'rhyolitic conglomerate'. Indeed, the size of the rounded to subrounded to ellipsoidal framework clasts that impart conglomeratic appearance to the rock are quite large, from 6 cm to as large as 30 cm; 8–12 cm more common. The very large clasts (>20–30 cm) are ellipsoidal to disc-shaped, or semi-rounded (figure 3c and d), and tend to be aligned along the vertical to sub-vertical N–S trending regional deformational fabric. Rounded to elliptical vesicles are observed on the clast surfaces (figure 3d). At places, cherty rhyolite fragments (∼ 15 cm) with rounded margin and tapering ends (spindle-shaped) are also observed (figure 3e). These clasts are massive rhyolite (figure 3f) and rhyolite tuff with phenocrysts/broken embayed phenocrysts of quartz and feldspar. Banded rhyolite clasts are also observed occasionally (figure 3g).

Overall, for bottom about 10–20 m of the conglomeratic part, the size of clasts increases, up to >25 cm (figure 2). The framework clasts (>20 cm) become less dominant for about next 10–15 m, where 8–20 cm clasts remain common and smaller (3–6 cm) angular clasts are less abundant. In the upper-most part of the deposit, larger clasts (>20 cm) again become fairly common; angular smaller ones (3–6 cm) less to sparse. Sarkar (1994) reported occurrences of 'pebbles' of minor amounts of older granites/granophyre, siltstone, cherts, etc., in the deposit presumably of basement derivation. This could, however, not be confirmed during this study.

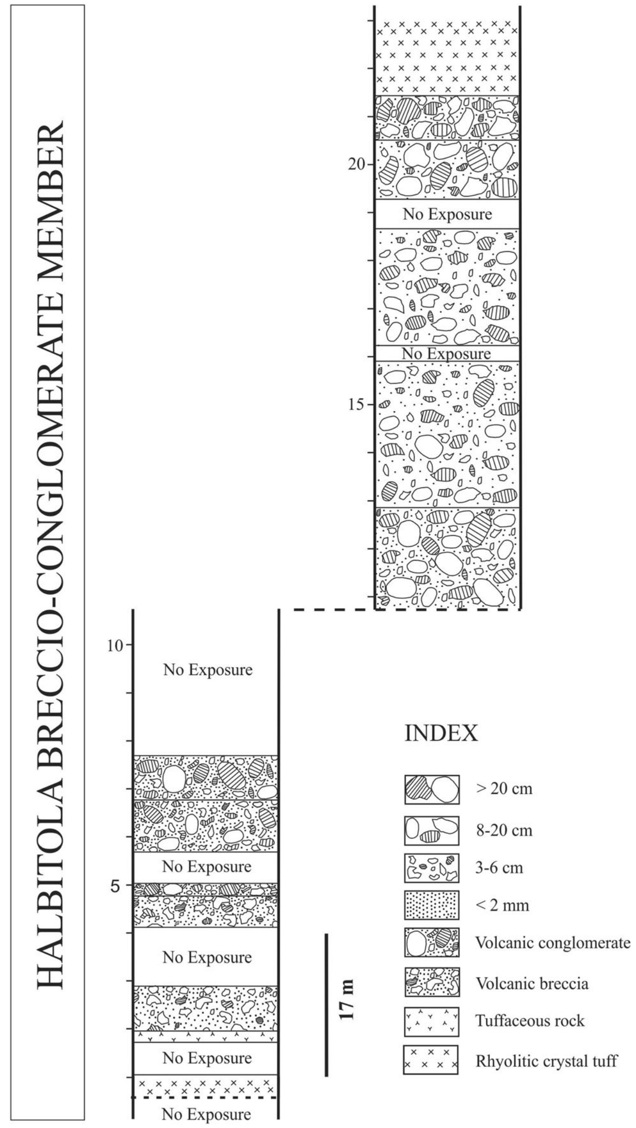

Figure 2. Approximately 125 m thick breccio-conglomerate section, showing variations of framework clast size and their angularities and/or roundness. Rhyolitic breccia (lower 30 m) has lapilli- to block-sized pyroclasts showing gradual transition finally to rhyolitic conglomerate (70–80 m) up the succession. Large clasts up to 30 cm in size in conglomerate part.

4. Petrography

The fragmental character characterises the deposit. As mentioned above, one of the striking features of the rock is the overall similarity in textures/micro-structures of volcanic clasts and rock matrix. The thin section petrography for large clasts and the matrix of the rock that hold the larger clasts are discussed in this section.

Table 2. *Occurrence in percentage of volcanic fragments in large clasts and matrix in the rock.*

	Large clasts					Rock matrix				
%	BC56	HBC/C6	HBC/C8	D18	D19A	BC55	M52	M31	BCC9	BCC3
Matrix	57.32	44.36	36.26	45.21	46.32	–	–	–	–	–
Crystals	25.29	26.52	27.95	7.56	5.22	14.92	13.53	7.85	15.87	6.85
Vitric	1.44	2.96	5.60	4.57	2.1	62.25	71.69	77.16	66.91	77.28
Lithics	15.96	26.16	31.09	43.66	46.36	22.83	14.78	15.09	17.23	15.87

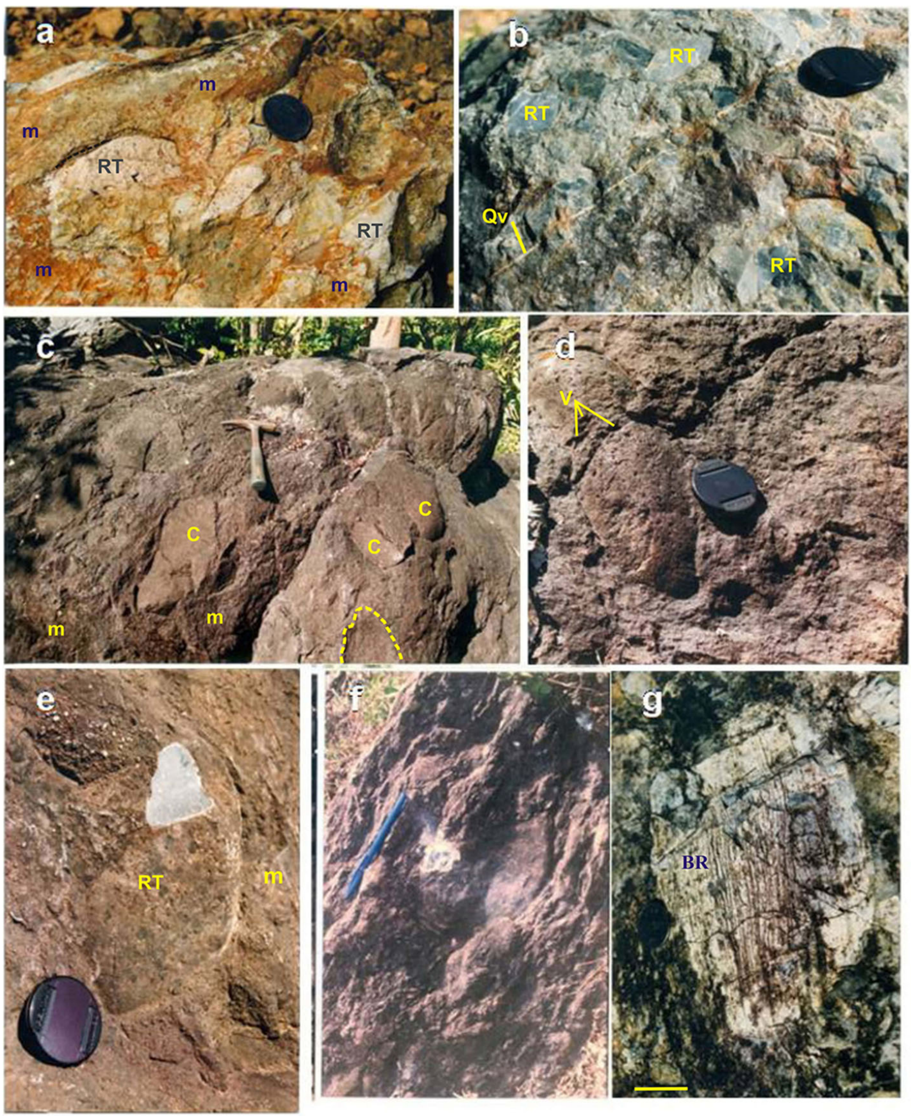

Figure 3. (**a**) Buff- to cream-buff-coloured angular rhyolite lapilli-tuff framework clasts (RT) set in fine-grained dense fragmental matrix (m) in lower-middle brecciated part. Clasts variably altered at places. (**b**) General view of rhyolitic breccia where very angular block-sized to lapilli-tuff (RT) fragments set in fragmental very coarse ash to lapilli-sized matrix. Fine quartz vein (Qv) cuts across the rock in the middle. (**c**) Large framework clasts (c) tend to round in the transition zone, though smaller pyroclastic fragments maintain angularity. Large clasts (middle-left) tend to taper at one end with curved margin on one side. (**d**) Well-rounded ellipsoidal bomb-sized framework (>20 cm) shows circular to elliptical vesicles; framework clast cut by a fracture in the middle. (**e**) Cherty white massive well-rounded conglomeratic bomb-sized clasts (RT) set in fragmental matrix (m). (**f**) Disc-shaped rhyolitic clast (15 cm) with tapering ends, related to shearing when still in molten state. Irregular N–S fabric observed in the adjacent fragmental matrix. (**g**) Very large fractured subangular banded rhyolite (BR) framework clast; clast shows irregular jagged and embayed margin (see lower right of photo). Camera lens cover diameter 6 cm in the respective photos.

4.1 *Larger clasts*

4.1.1 *Framework grains*

Under the microscope, framework clasts (>6 cm) irrespective of the extent of their angularity have crystals of quartz, feldspars set in essentially finer vitroclastic to microcrystalline devitrified pumiceous matrix (figure 4a and b); matrix constitutes nearly 60% of the framework clasts. The modal count percentage of different constituents (e.g., crystals, vitrics, lithics and matrix) for selected framework clasts is presented in table 2.

Quartz and feldspar (up to 27%), the most abundant crystals are often broken and usually <2 mm in size. Broken crystals that are opaque are also present. Euhedral to subhedral feldspars with well-developed prismatic faces show embayed to serrated margins (figure 4a). Feldspars (albitic plagioclase) appear frosted and show albite and carlsbad twinning; k-feldspar is orthoclase. Quartz characteristically shows unitary extinction. Rounded to oval-shaped quartz frequently show embayed margins (figure 4c). Embayed margin is likely developed due to magmatic resorption and corrosion. Crystals of quartz are internally fractured; occasionally conchoidal fractures observed (figure 4c). Fractures are cross-cutting crystals of quartz, often intersecting melt inclusions (now devitrified) as similar to adjacent devitrified matrix and/or embayed margins. Thin selvages of fine-grained devitrified matrix also occur along the fractures.

Lithic clasts mainly comprise devitrified tuff of rhyolitic compositions (figure 4d), and are petrographically classified as lithic tuff to lithic-crystal tuff (figure 5), as similar to the rock types described from the main body of the Bijli Rhyolite (Sarkar 1957, 1958; Mukhopadhyay *et al.* 2001; Sensarma and Mukhopadhyay 2003; Sensarma *et al.* 2004). Accessory minerals include zircon, sphene, iron-oxide with chlorite and calcite.

4.1.2 *Matrix*

Matrix of the large lithic clasts comprises cryptocrystalline largely equant semi-circular dense microcrystalline grey-coloured cellular to filamentous devitrified pumice (figure 4e). The domains of micro- to cryptocrystalline aggregate are best recognised with rotation of the microscope stage under cross-nicol. Owing to extreme fineness of the microlites/crystallites, the mineralogy of the aggregate mass is not resolvable under the microscope. However, on the basis of average optical properties, pumiceous grains appear to be made up of quartz–feldspar micro- to cryptocrystalline aggregates.

The domanial pumiceous grains tend to be elongated at places (figure 4e and f). The elongation of dense microcrystalline aggregates (pumice) imparts a directional fabric in the matrix. Well-developed small euhedral feldspar is seen aligned to this fabric at places (figure 4f). Devitrified pumice remains attached and sometimes coalesce on feldspar boundary. Under higher magnification, the semi-circular to elongated pumiceous domains devitrified to coarser aggregates at high temperature shows intricate quartz–feldspar aggregates with tiny, but remarkably intact, vesicular structures giving delicate porous spongy appearance (figure 4g).

Few tiny crystals of quartz and feldspar ± chlorite are also present in the matrix. Blebs and flakes of opaque and dark green biotite (0.01–0.02 mm) occur with/without chlorite. Also, alternate layers of comparatively coarser and extremely fine quartz–feldspar aggregate are discernible at places in the matrix (figure 4e). Sericitisation in the finer quartz–feldspar bearing layers are more common that aid in distinguishing it from the layers with coarser quartz–feldspar aggregates.

4.2 *Matrix of the rock*

The matrix of the rock is predominantly a vitric-tuff (figure 5) with presence of crystals and lithics, the latter especially in the lower brecciated part. Vitric grains are abundant and constitute up to 75% of the matrix. The representative modal data of the matrix of the rock is presented in table 2. The general petrographic character of the matrix of the rock is discussed below.

4.2.1 *Fragments in matrix*

Vitric fragments are the dominant component in the matrix (figure 6a). Under higher magnification, subrounded patches/domains show evidence of high-temperature devitrification in the form of slender crystallite of quartz–feldspar aggregate (figure 6b); tiny vesicles recognised, occasionally filled with chlorite, within these intricately devitrified materials. Extensive devitrification makes

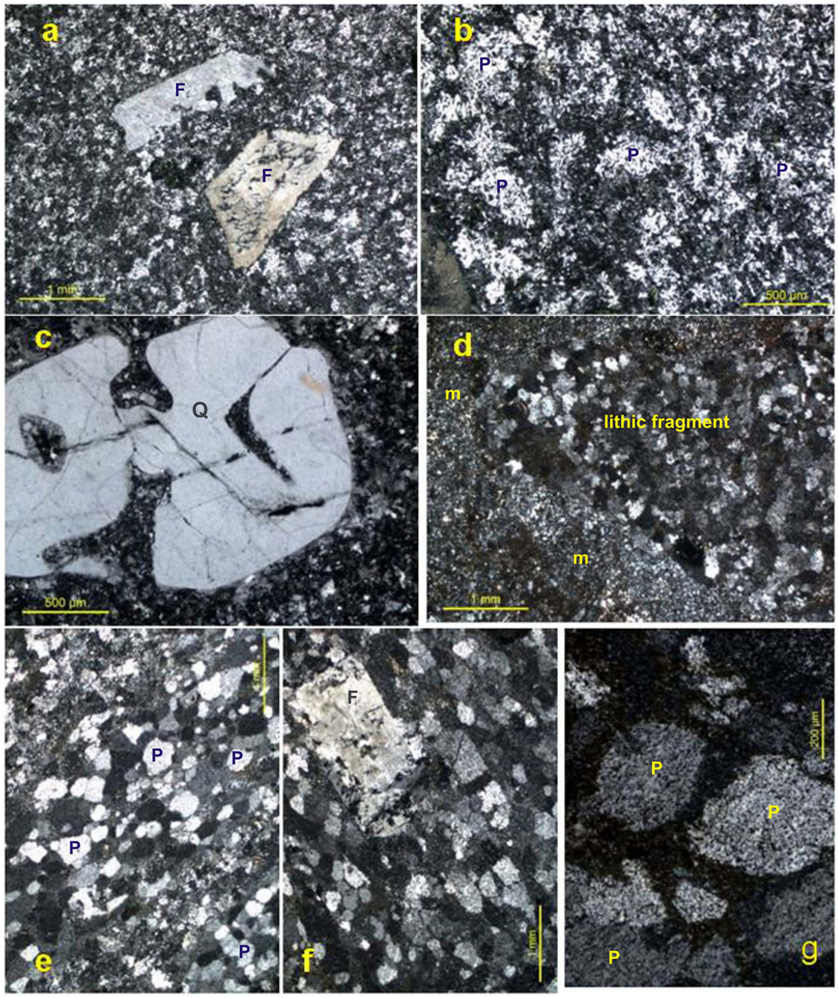

Figure 4. Photomicrographs of large framework pyroclasts: (**a**) well-developed euhedral feldspars (F) set in dense microcrystalline devitrified tuff matrix; frosted appearance of embayed albite (upper left). Corrugated margins of zoned feldspar (lower right); internal part show reaction microstructures. (**b**) Under higher magnification equant subrounded devitrified pumiceous domains (P) of microcrystalline reticulate aggregates of quartz–feldspar; pumice occasionally tend to elongate. (**c**) Oval-shaped quartz (Q) with embayed margins showing unitary extinction; occasionally showing conchoidal fractures. (**d**) Subrounded devitrified rhyolitic tuff fragment (lithic) in finer dense cryptocrystalline matrix (m); tuff fragment comprises pumice devitrified into fine quartz–feldspar aggregates. (**e**) Alternate subtle micro-layers of comparatively coarse and extremely fine devitrified quartz–feldspar aggregate of ash-sized pumiceous fragments (P) in matrix. (**f**) Devitrified pumice (vitric) ash and well-developed euhedral phenocryst feldspar (F) develop directional alignment likely indicate incipient flowage; devitrified pumice (vitric) ash also attached to euhedral feldspar (F). (**g**) Under higher magnification, semicircular to elongate pumiceous domains (P) show intricate coarser quartz–feldspar aggregates with tiny vesicles. All photos taken in cross-nicol.

their recognition difficult indeed, causing estimation of its original abundance almost impossible. Nevertheless, the conservative estimate of modal count suggests vitric component comprise at least 50–60%, and may go up to 75%.

Lithic fragments constitute ≤20% within the matrix of the rock. The lithic fragments (figure 6c) are similar to those (vitric tuff) observed in the Bijli rhyolites (see Mukhopadhyay *et al.* 2001). These are generally angular to subangular and have variably distinct margins, which makes it difficult to recognise against the fine-grained devitrified pumice. The lithic fragments vary in size (<1 to >2 mm). An interesting lithic fragment is the presence of micro-phyric basaltic clasts, in which plagioclase micro-laths are set in a cryptocrystalline brown to greenish brown extremely fine devitrified glass ± chlorite (figure 6d and e) giving rise to vitrophyric texture. The mafic clasts show subrounded crenulate margins. The presence of green to brownish green tiny chlorite is common in the matrix interpreted to be altered mafic glass.

The texturally different rhyolitic lithic fragments (pyroclastic tuffs) recognised are: (i) pumice-rich lithic fragment which volumetrically constitutes a major portion, has microgranular to microfilament

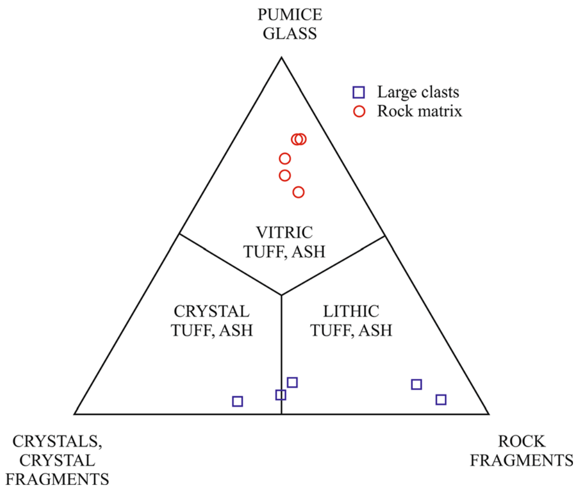

Figure 5. Petrographic classification (after Schmid 1981) shows lithic-tuff to lithic-crystal tuff for large fragment clasts and vitric tuff for matrix of the rock.

quartz and feldspar (devitrified products of silicic glassy material) as the principal constituents. Occasionally sericite is also present. The worm-like microfilament of quartz–feldspar aggregates represent devitrified shards within the tuff fragments. (ii) Lithic fragments of pumiceous tuff with included lithic fragments of similar type are the other type (figure 6f). The included lithic fragments are, however, relatively finely devitrified and show subrounded grain boundaries against the comparatively coarsely devitrified host. Fragments of granophyric rhyolite are also included within the coarsely devitrified lithic clast. (iii) Very coarsely devitrified tuff is another lithic component present in the matrix. (iv) Plagioclase-phyric silicic lithic clasts having large tabular to lath-shaped plagioclase (0.5–0.9 mm) ± subangular quartz phenocrysts set in a very fine-grained devitrified matrix made up of fine quartz + acicular sericite + fine biotite + opaque. Plagioclase phenocrysts are altered, yet show albite twinning. Subangular quartz phenocrysts in this type of lithic fragment are principally noticed in the matrix of the conglomeratic part of the deposit.

Isolated *crystals* of quartz and feldspar, sometimes broken, constitute about 5–10% of the matrix of the rock (figure 6a, f and g). Crystals (0.4–1.2 mm) are euhedral to subhedral and poorly sorted. With increase in size, roundness improves in quartz. Quartz is inclusion free, and also shows embayed margins. Some crystals of quartz exhibit conchoidal fractures and undulose extinction. The individual feldspars (0.4–1 mm) are variably sericitised. Well-developed rhombic euhedral sanidine show unitary extinction (figure 6a). Feldspars have regular crystal faces (figure 6f and g); margins of the broken portion are occasionally jagged (figure 6g). Feldspars are multiply twinned and also occasionally occur in clusters. Triangular twinned feldspars have straight and subrounded margins at places; twin planes terminating abruptly against grain boundaries (figure 6f). Clusters of twinned feldspar with sharp margins are found in an interlocking arrangement with the micro-phyric basalt rock fragments (figure 6e). Quartz is inclusion free, and also shows embayed margins. Isolated irregular to patchy opaque grains is the other crystals present in the matrix of the deposit.

5. Discussion

The recognition of pyroclastic and/or epiclastic (reworked resedimented) deposits, particularly in deformed and metamorphosed ancient volcanic successions are difficult indeed, sometimes even uncertain (see McPhie *et al.* 1993). Yet, recognition of delicate pumice in the Precambrian rocks are sometimes possible (e.g., see Müller *et al.* 2000 and references therein), and that depends to a large extent on post-depositional history of the deposit. In the current study, it follows from the above descriptions that the rock comprises essentially of rhyolitic lithic fragments of diverse textural types, vitric grains (pumice shards) and crystals. Angular to subangular lithic (rhyolite tuff) fragments set in a microcrystalline fragmental to aphanitic rhyolitic matrix imparts an overall fragmental texture. The mineralogical composition and textural make up clearly help identify the rock to be of explosive silicic volcanic origin, and therefore, non-genetically, a volcaniclastic deposit. However, whether this volcaniclastic rock is made up essentially of primary volcanic particles ejected during Bijli volcanism and also emplaced by primary volcanic processes and/or rapid sedimentation of freshly erupted texturally unmodified particles or epiclastic processes is of importance, as discussed below.

5.1 *Pyroclastic origin*

General massive character of the deposit, lack of bedforms, high particle concentrations, fine-to-coarse devitrification of rounded to subrounded vesicular ash-sized pumice, presence of large

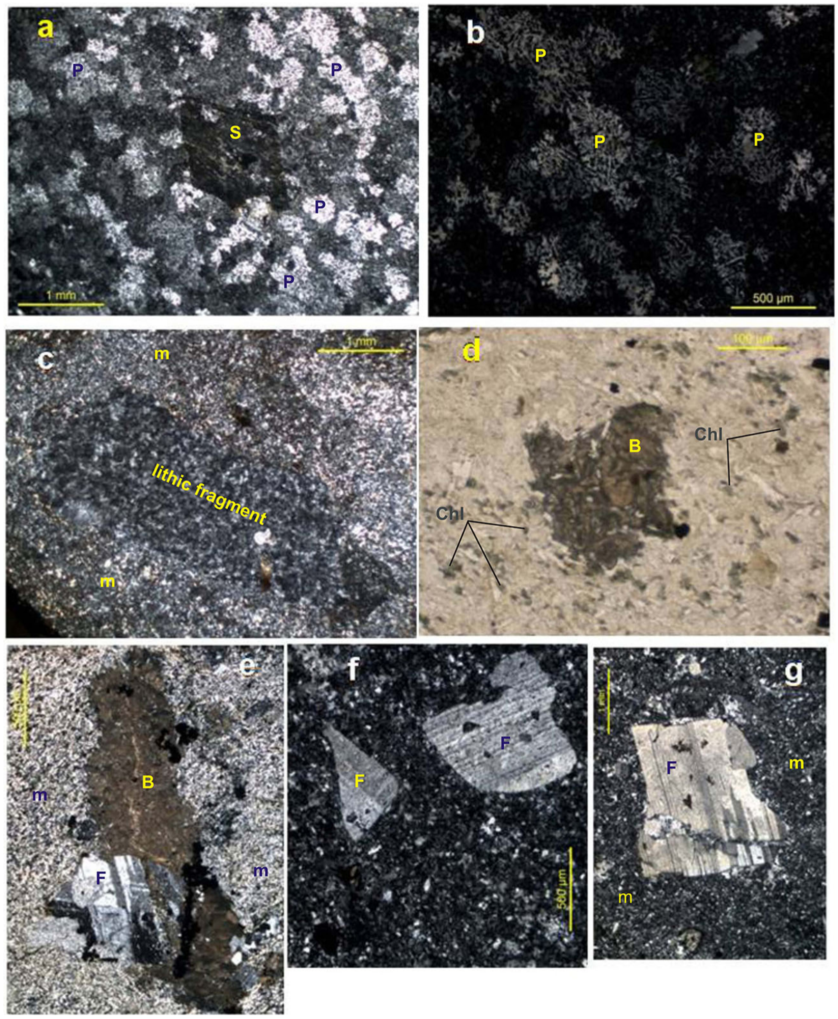

Figure 6. Photomicrographs of matrix of the rock. (**a**) Devitrified pumice ash (P) occurs as domains of microcrystalline quartz–feldspar aggregate; occasionally coalescing devitrified pumice (vitric) show no to incipient welding; euhedral rhombic sanidine shows unitary extinction. (**b**) Under higher magnification, slender micro-crystalline quartz–feldspar aggregate in devitrified pumiceous grains (P). (**c**) Angular rhyolite tuff fragment (lithic) set in very fine dense aphanitic matrix (m). (**d**) Micro-plagioclase-phyric basalt enclave with rounded corners (B) in rhyolitic matrix; vitrophyric texture with fine devitrified brown glass in enclave groundmass; chlorite-rich brownish green tiny patches (Chl) altered basaltic glass. Photo taken in plane polarised light. (**e**) Interlocking arrangement of cluster of well-developed euhedral feldspar (F) of silicic volcanic rocks and the same basalt enclave (B). (**f**) Twinning in triangular feldspars (F) terminating against straight and slightly subrounded margins. (**g**) Broken euhedral feldspar (F); crystal margins jagged; part of crystal slightly rotated after breakage, set in finer matrix (m). Photos taken in cross-nicol, unless otherwise stated.

number of angular to rounded to ellipsoidal vesicular volcanic blocks/bomb-sized (>8 cm, up to 30 cm) clasts, commonly poorly sorted nature of the deposit, vitrophyric matrix, euhedral broken crystals of quartz with embayed resorbed margins and unitary extinction, well-developed multiply twinned tabular euhedral feldspars including sanidine – all overwhelmingly support the deposit irrefutably linked to explosive silicic Bijli volcanism, and thus of pyroclastic origin. The cognate lithic clasts of rhyolitic tuff, rhyolite clasts with granophyric matrix and glassy or cryptocrystalline devitrified pumiceous rhyolite are all of penecontemporaneous origin, particularly for being part of LIP rhyolite volcanism (Bijli Rhyolite). Also, it is equally important to note that lack of evenly porphyritic texture, lack of uniformity of euhedral crystals and their size, mineralogy and proportions exclude the possibility for a lava flow origin for the deposit.

5.2 *Type of pyroclastic deposit*

Although vitric fragments (pumice shards) are present both in the clast and much more abundantly in rock matrix, not much welding or incipient coalescence of vitric particles at places is observed in either component. However, the pumice fragments along with the well-developed euhedral phenocrystic feldspar occasionally tend to develop directional alignment (figure 4f). Since the curved boundaries of the pumiceous fragments always maintain parallelism and do not cut across by any fracture/foliation, it is likely that the directional alignment could indicate a primary incipient flowage condition. The subtle alternation of comparatively coarser and finer devitrification zone may suggest differential thermal condition during devitrification of the pumice fragments (figure 4e).

Monolithologic unsorted character and small volume of the breccio-conglomerate deposit, large cognate clasts emplaced as blocks (in brecciated part) and bombs (in conglomeratic part) of the same magma type, predominance of ash-sized matrix, non-welded to incipiently coalescence (incipiently welded) nature of pumice-all suggest the deposit likely related to overall unwelded to incipiently welded pyroclastic flow (ignimbrite) emplacement. Antecrysts of euhedral broken quartz and feldspar displaying disequilibrium features such as magmatic rounding and resorption, which crystallised from earlier silicic liquid, but are not in equilibrium with the host silicic liquid (groundmass), unlike xenocrysts, represent part of the same LIP rhyolite system. The possibility of the crystals displaying disequilibrium features being xenocrysts are ruled out as xenocrysts would have been mineral phases incompatible with, or atypical of the host silicic magma composition, as they get incorporated from foreign source. On the other hand, phenocrysts remain in equilibrium with the host silicic liquid (groundmass). Antecryst entrainments are indeed common features of rhyolites from caldera-forming eruptions in continental settings (Storm *et al.* 2011).

Cognate lithic pyroclasts have similar looking pumice as those in matrix of the rock, and are therefore likely represent portion of the magmas chilled against the caldera wall and/or magmas crystallised little earlier as part of the same Bijli system, and co-magmatic with other juvenile pyroclasts. The lithic clasts differ texturally, perhaps depending on their source. In lava collapse situation, in addition to the same type of phenocrysts, more banded rhyolite lava fragments would have also been encountered, contrary to what is observed here. Also, lithic tuff fragments are generally uncommon to sparse in rhyolite lava flows (cf. McPhie *et al.* 1993). The absence of accidental clasts of any other rock type in the rock may also preclude their origin from lava flows.

Broken crystals provide evidence of disruption of magma during or prior to extraction from the reservoir (e.g., Maughan *et al.* 2002). When combined with micro-vesicularity of the pumice clasts, these textural characteristics suggest that vesiculation may have played a role in the eruption process (Gottsmann *et al.* 2009).

The textural relations, including rounded margins of the micro-enclaves of basalt are in interlocking arrangement with well-developed euhedral feldspars or cluster of feldspars (figure 6d and e). The presence of vitrophyric texture in the basalt micro-enclave may suggest rapid quenching with a sudden drop in temperature during mafic magma eruption, expected in volcanic setting. Also, microvesicles of rhyolitic pumice filled with chlorite-like material interpreted to be of devitrified basaltic glass. The textural relations of mingling of silicic–mafic magmas, including the rounded/subrounded margins of the basaltic micro-enclaves, imply that the basaltic melts were incorporated into rhyolite while both were in a molten state. This is suggestive of mafic recharge before the explosion. The overlapping ratios of immobile and mantle-incompatible elements, e.g., Sm/Nd and Zr/Y values in the Bijli rhyolites and immediately overlying basalts (Pitepani basalts) occurring in spatial proximity to the breccio-conglomerate deposit in the area (figure 1), and comparison with experimental partial melts compositions and petrological modelling (Sensarma *et al.* 2004) confirm rhyolite–basalts interactions in their molten states giving rise to hybrid Bijli rhyolites (see also Sensarma 2007).

5.3 *Relation to subaerial Bijli volcanism*

Since the deposit is petrogenetically linked and indeed part of the Bijli volcanism, it then follows that the breccio-conglomerate deposit accumulated synchronously with the ignimbrites, the major component of the Bijli explosive volcanism, likely as near-vent facies. The voluminous Bijli Rhyolite (>8000 km^3) (Sensarma *et al.* 2004) comprises high-grade rheoignimbrites, ignimbrites, welded tuff, volcanic breccia (see Mukhopadhyay *et al.* 2001). Such silicic pyroclastic breccias/breccio-conglomerate with rhyolitic lithic fragments of variable textures and microstructures likely indicate caldera collapse associated with Bijli Rhyolite explosion. The most remarkable characteristic of the rock is that both clasts and matrix are petrographically and compositionally similar suggesting coeval and syn-eruptive crystallisation of both the fractions from the magma. Similar suggestion is also put forwarded for compositionally identical clasts and matrix of a welded ignimbrite in Gran Canaria (Freundt and Schmincke 1995). Coarse angular rhyolitic blocks common in the brecciated part of the deposit may indicate near vent origin.

Structures in the deposit record only the final transport stage, but earlier transport modes can be inferred from various features including clast shape, abundance and sorting. The subaerial explosive eruptions led to the formation of silicic high-grade rheoignimbrites, ignimbrites, welded tuff, volcanic breccia (Bijli rhyolites; Mukhopadhyay *et al.* 2001; Chakraborty *et al.* 2021).

Lack of conspicuous bedforms and internal stratification in the deposit do not satisfy it as fall deposit (Wilson 2008). Of course, it is very difficult to ascertain at this time whether original fine internal stratification, if any, is obliterated due to deformation and metamorphism in such an ancient volcanic deposit. Given uncertainty, eruption of abundant pyroclastic ejecta, non-heterolithic character, absence of erosional epiclastic material, large size and angularity of the lithic clasts that were derived from the subaerial Bijli volcanism, combine together to indicate that the breccio-conglomerate deposition took place in similar subaerial condition. The gradual lithological change of the deposit from the brecciated part to the upper conglomeratic part could be related to significant changes in slopes that were developing in such volcanic environment, as discussed below.

5.4 *Cause of rounding of larger clasts*

It is mentioned above that the rhyolitic breccio-conglomerate deposit is earlier considered as a special class of polymictic conglomerate of epiclastic origin (Sarkar 1956, 1957, 1958). It is conceivable that the volcanic clasts of epiclastic origin would require presumably prolonged period of transportation as in a normal sedimentary system to get better rounded. The rounding of the pyroclastic clasts in an oligomictic tuffaceous conglomerates in the Dalma metavolcanic range in the Singhbhum district (eastern India) is also attributed to reworking of coarse volcanic materials (Gupta *et al.* 1977).

In contrast, in this case, coexistence and gradational transition of angular and spindle-shaped volcanic fragments (blocks and bomb-sized particles) of overall similar petrography cannot be explained by action of normal epiclastic process long after volcanism. Ash-sized rounded to near-rounded shape of unstable delicate pumice grains, now occur as domainal patches of devitrified felsic microcrystalline aggregates, would have completely been destroyed beyond recognition during prolonged transportation and/or reworking. Simultaneous cooling and crystallisation of both rounded clasts and matrix in the rock and lack of bedforms in the deposit and unmodified textures including lack of large-scale alteration of volcanic particles in both clasts and matrix particles do not support epiclastic transportation regime either. Therefore, an alternative mechanism of transportation is called for, particularly to account for the rounding of the rhyolitic volcanic clasts, yet retain unmodified textural characteristics.

Fragmental nature and simultaneous crystallisation and cooling of both clasts and matrix of the deposit indicate that pyroclastic fragments were formed, supplied and transported together along steep slopes commonly available in explosive volcanic terrains, particularly in post-caldera collapse setting and/or caldera wall/floor destabilisation (cf. Gooday *et al.* 2018). Initial high temperatures of the ejected volcanic fragments (e.g., lithics and pumice), while still molten/partly molten and hence plastic state, aerodynamically developed smooth curved outer surfaces because of surface tension, resulting into rounding into ellipsoidal to smooth fluidal surfaces in a shorter interval of time, geologically coeval to volcanism. Larger clasts with more magmatic mass possibly retained heat and therefore remained hot enough inside and thereby plastic, were conducive to impart better rounding of the larger clasts leading to conglomeratic appearance to the rock. Local shearing, when still in molten state, may have possibly led to asymmetry in curvature and length of some clasts (figure 3e).

It is also conceivable that interactions of fragments amongst themselves during rapid movement along high gradient slopes, and abrasion along the floor in unstable caldera-related volcanic environment may also have partly contributed to rounding of volcanic clasts. The close spatial and contemporaneous relations of breccio-conglomerate to the explosive Bijli

Rhyolite and silicic–mafic magma interactions (see section 5.2) also argue for shorter duration of emplacement for the fragments to volcanism. The high content of ash-sized particles, occasional subrounded nature of some of the cognate lapilli- to bomb/block-sized lithic clasts and the presence of crystals with rounded margins in a pyroclastic deposit is also considered as evidence for mechanical abrasion in the depositing mass (Freundt and Schmincke 1992). Thin micro-crystalline quartz–feldspar aggregate (devitrified pumice fragments), occasionally adhering to the crystals may also indicate some abrasion of particles during the emplacement of the deposit.

Textural evidence of mafic melts interactions in the core unlike near the margins of euhedral volcanic feldspar (figure 4a) is commonly interpreted to reflect intrusion of mafic magma into the system in the latter part of crystal growth. Indeed, only decadal time gap is estimated for dacites, andesites and quenched mafic inclusions (mafic magma) formed during mafic–silicic magma interactions (Costa and Chakraborty 2004).

6. Stratigraphic implications

Considering prolonged period of transportation in a normal sedimentary system imparting better roundness to volcanic fragments, Sarkar (1957, 1958, 1994) inferred the presence of 'non-conformity' at the base of this deposit within the Bijli Rhyolite. Also, perhaps because of large eruptions of extremely contrasting highly silicic (Bijli Rhyolite) and mafic volcanism (Pitepani basalts) within his Nandgaon group, Sarkar also suggested an unconformity between the 'rhyolitic conglomerate' and the overlying Pitepani basalts (see table 1). Gupta *et al.* (1977) also suggested a disconformity at the base of the volcanic conglomerate deposit in Singhbhum by invoking an eruptive phase, followed by prolonged reworking of the debris within the basin or from sources to the depositional site.

The stratigraphic relations of the litho-units in the easterly dipping western limb of the regional 'Sitagota syncline' suggest that the breccio-conglomerate rock occurs towards the upper part of the Bijli Rhyolite, and thus emplaced at a later stage of the large Bijli event following a certain level of silicic magma withdrawal. It is discussed above that the basaltic melts were incorporated into rhyolite while both were in molten state. Detailed geochemical and petrogenetic studies of the Bijli rhyolites and siliceous high-Mg basalts (Pitepani basalts) also confirmed rhyolite–high-Mg basalt interactions in the province (Sensarma *et al.* 2002, 2004; Sensarma 2007), and thus near-coeval silicic–mafic volcanism too. Since the formation of explosive volcanic particles and their deposition forming breccio-conglomerate deposit is genetically linked and coeval to LIP rhyolite volcanism (Bijli Rhyolite) in the province, no unconformable relation between the two could exist.

Owing to the lithologic distinctiveness within the Bijli Rhyolite, the breccio-conglomerate deposit is given a separate status, and assigned the rank of *member* (Hedberg 1976, p. 33; see Sensarma and Mukhopadhyay 2014), and called the Halbitola Rhyolitic breccio-conglomerate member within the Bijli Rhyolite.

Therefore, combining field relations, petrography and earlier geochemical study do not call for a large time gap (unconformity/non-conformity) between the Bijli rhyolites and the silicic breccio-conglomerate deposit on one hand, and the silicic breccio-conglomerate deposit and the overlying Pitepani basalts on the other, pointing to the development of a continuous LIP volcanic stratigraphy (Sensarma and Mukhopadhyay 2014 and references therein; see also table 1 for comparison with Sarkar's stratigraphy). In general, the absence of internal erosion surfaces or sedimentary deposits produced by epiclastic processes, the deposition of pyroclastic breccio-conglomerate deposit within the Bijli Rhyolite may have taken place within a period of days (cf. Christiansen 1979, 2001) to only decadal time duration (cf. Costa and Chakraborty 2004).

7. Summary and conclusions

A ∼2.5 Ga volcaniclastic conglomerate deposits in the Dongargarh LIP was earlier interpreted to have been derived by significant reworking during transport of primary volcanic particles prior to deposition, but long after volcanism (epiclastic). However, common occurrence of large angular (breccias) and rounded to ellipsoidal-shaped (conglomerate) cognate lithic fragments (blocks and bomb-sized), equant-rounded pumice shards, euhedral resorbed and embayed broken quartz and feldspar, simultaneous cooling and crystallisation of both rhyolitic clasts and matrix, general massive and texturally unmodified character, lack of bedforms and post-depositional structures in the deposit support for a pyroclastic origin, related to Bijli volcanism contrary to an epiclastic or a reprocessed origin, for the breccio-conglomerate deposit within a subaerial LIP rhyolite.

Rounding of pyroclasts may have taken place in shorter time, perhaps within days/months. Supply of pyroclastic fragments likely controlled by the caldera collapse during Bijli volcanism. Hot molten volcanic ejecta in plastic state, was aerodynamically conducive for surface rounding that imparted conglomeratic appearance to the rock, not attributable to reprocessing of fragments long after volcanism. Mechanical interactions of the pyroclasts along steep slopes common in such volcanic environment, however, also partly contributed to rounding of clasts.

Evidence of silicic–mafic melts interactions in the province including the breccio-conglomerate also suggests no fundamental and abrupt change in magmatic/depositional environment either. Near-coeval silicic (Bijli) and mafic (Pitepani basalts) magma interactions reiterates a continuous volcanic stratigraphy (Dongargarh group) for the Dongargarh LIP, consistent with the general stratigraphic framework of LIPs worldwide.

Acknowledgements

Authors acknowledge Prof Dhruba Mukhopadhyay (formerly of the University of Calcutta), for introducing SS to the fascinating geology of the Dongargarh province long back, Prof N V Chalapathi Rao and Prof J S Ray (the guest editors) for the invitation to contribute to this special volume in memory of late Prof Gautam Sen, an acclaimed petrologist of our time, Department of Geology, University of Lucknow for support. The paper is benefitted from the comments of two anonymous reviewers.

Author statement

First author: Fieldwork; formulation of the idea, overall technical supervision. Both authors: Participated in thin-section petrography study, interpretation, writing and preparation of the final manuscript.

References

Bryan S E, Peate I U, Peate D W, Self S, Jerram D A, Mawby M R, Marsh J S and Miller J A 2010 The largest volcanic eruptions on Earth; *Earth Sci. Rev.* **102** 207–229, https://doi.org/10.1016/j.earscirev.2010.07.001.

Cas R A F and Wright J V 1987 *Volcanic successions: Modern and ancient*; Allen and Unwin, London, 528p.

Chakraborty M, Debnath S and Mahapatro S N 2021 Lithofacies analysis of volcanics and volcaniclastics of an ancient volcanic terrain with signatures of subaerial plinian volcanism: An example from Neoarchaean–Palaeoproterozoic Nandgaon group, Bastar craton, central India; *J. Earth Syst. Sci.* **130** 145, https://doi.org/10.1007/s12040-021-01656-5.

Chakraborty T and Sensarma S 2008 Shallow marine and coastal eolian quartz arenite in the Neoarchaean–Palaeoproterozoic Karutola formation, Dongargarh volcano-sedimentary succession, central India; *Precamb. Res.*, https://doi.org/10.1016/j.precamres.2007.07.024.

Cheng L, Trenberth K E, Fasullo J, Boyer T, Abraham J and Zhu J 2017 Improved estimates of ocean heat content from 1960 to 2015; *Sci. Adv.* **3(3)**, https://doi.org/10.1126/sciadv.1601545.

Christiansen R L 1979 Cooling units and composite sheets in relation to caldera structure; In: *Ash-flow tuffs* (eds) Chapin C E and Elston W E, *Geol. Soc. Am. Spec. Pap.* **180** 29–42.

Christiansen R L 2001 Quaternary and Pliocene volcanism of the Yellowstone Plateau region of Wyoming, Idaho, and Montana: *U.S. Geol. Surv. Prof. Pap.* **729-G** 143.

Costa F and Chakraborty S 2004 Decadal time gaps between mafic intrusion and silicic eruption obtained from chemical zoning patterns in olivine; *Earth Planet. Sci. Lett.* **227** 517–530, https://doi.org/10.1016/j.epsl.2004.08.011.

Deshpande G G, Mahobey N K and Deshpande M S 1990 Petrography and tectonic setting of Dongargarh volcanics; *Geol. Surv. India Spec. Publ.* **28** 260–288.

de Silva S 2008 Arc magmatism, calderas, and supervolcanoes; *Geology* **36(8)** 671–672, https://doi.org/10.1130/focus082008.1.

Fermor L L 1934 General report for 1934; *Rec. Geol. Surv. India* **67(1)** 88p.

Fermor L L 1935 General report for 1934; *Rec. Geol. Surv. India* **68(1)** 91p.

Fisher R V 1966 Rocks composed of volcanic fragments and their classification; *Earth Sci. Rev.* **1** 287–298.

Fisher R V and Smith G A 1991 Sedimentation in volcanic settings; *SEPM Spec. Publ.* **45** 1–5.

Fiske R S 1969 Recognition and significance of pumice in marine pyroclastic rocks; *GSA Bull.* **80(1)** 1–8, https://doi.org/10.1130/0016-7606(1969)80[1:RASOPI]2.0.CO;2.

Freundt A and Schmincke H-U 1992 Abrasion in pyroclastic flows; *Geol. Rundsch.* **81(2)** 383–389.

Freundt A and Schmincke H-U 1995 Eruption and emplacement of a basaltic welded ignimbrite during caldera formation on Gran Canaria; *Bull. Volcanol.* **56** 640–659, https://doi.org/10.1007/BF00301468.

Ghose N C, Chatterjee N and Windley B F 2016 Subaqueous early eruptive phase of the late Aptian Rajmahal volcanism, India: Evidence from volcaniclastic rocks, bentonite, black shales, and oolite; *Geosci. Frontiers* **8** 809–822, https://doi.org/10.1016/j.gsf.2016.06.007.

Ghosh J G 2004 Geochronological constraints on the evolution of the Kotri linear belt and its basement; *Rec. Geol. Surv. India* **136(2)** 24–26.

Gooday R J, Brown D J, Goodenough K M and Kerr A C 2018 A proximal record of caldera-forming eruptions: The stratigraphy, eruptive history and collapse of the Palaeogene Arran caldera, western Scotland; *Bull. Volcanol.* **80**(**70**), https://doi.org/10.1007/s00445-018-1243-z.

Gottsmann J, Lavallée Y, Martí J and Aguirre-Díaz G 2009 Magma-tectonic interaction and the eruption of silicic batholiths; *Earth Planet. Sci. Lett.* **284(3–4)** 426–434, https://doi.org/10.1016/j.epsl.2009.05.008.

Gupta A and Basu A 2000 North Singhbhum proterozoic mobile belt eastern India – A review; *Geol. Surv. India Spec. Publ.* **55** 195–226.

Gupta A, Basu A and Singh S K 1977 Occurrence of a pyroclastic Conglomerate in Dalma Metavolcanics, Singbhum district, Bihar; *Indian J. Earth Sci.* **4**(**2**) 1601–1668.

Halder M, Paul D and Sensarma S 2021 Rhyolites in continental mafic large igneous provinces: Petrology, geochemistry and petrogenesis; *Geosci. Frontiers* **12**(**1**) 53–80, https://doi.org/10.1016/j.gsf.2020.06.011.

Hedberg H D (ed.) 1976 *International stratigraphic guide – A guide to stratigraphic classification, terminology and procedure*; John Wiley & Sons, New York, 200p.

Krishnamurthy P, Sinha D K, Rai A K, Seth D K and Singh S N 1990 Magmatic rocks of the Dongargarh supergroup, central India – Their petrological evolution and implications on metallogeny; *Geol. Surv. India Spec. Publ.* **28** 303–319.

Manikyamba C, Santosh M, Chandan Kumar B, Rambabu S, Tang L, Saha A, Khelen A C, Ganguly S, Singh Th D and Subba Rao D V 2016 Zircon U–Pb geochronology, Lu–Hf isotope systematics, and geochemistry of bimodal volcanic rocks and associated Granitoids from Kotri belt, central India: Implications for Neoarchean–Palaeoproterozoic crustal growth; *Gondwana Res.* **38** 313–333, https://doi.org/10.1016/j.gr.2015.12.008.

Maughan L L, Christiansen E H, Best M G, Gromme C S, Deino A L and Tingey D G 2002 The oligocene lund tuff, great basin, USA: A very large volume monotonous intermediate; *J. Volcanol. Geotherm. Res.* **113(1–2)** 129–157, https://doi.org/10.1016/S0377-0273(01)00256-6.

McPhie J, Doyle M and Allen R 1993 Volcanic textures: A guide to the interpretation of textures in Pyroclastic Rocks. Hobart Australia: CODES Key Centre, University of Tasmania, GPO Box 252C, Hobart, Tasmania 7001, 196p.

Mukhopadhyay J, Ray A, Ghosh G, Medda R A and Bandyopadhyay P P 2001 Recognition, characterization and implications of high-grade silicic ignimbrite facies from the Palaeoproterozoic Bijli rhyolites, Dongargarh supergroup, central India; *Gondwana Res.* **4** 519–527, https://doi.org/10.1016/S1342-937X(05)70351-8.

Müller W, Chown E H and Thurston P C 2000 Processes in physical volcanology and volcaniclastic sedimentation: Modern and ancient; *Precamb. Res.* **101** 81–85, https://doi.org/10.1016/S0301-9268(99)00095-9.

Ramachandra H M and Roy A 1998 Geology of intrusive granitoids with particular reference to Dongargarh granite and their implication on tectonic evolution of the Precambrian in central India; *Indian J. Geosci. (formerly Indian Minerals)* **52** 15–32.

Rooney T O, Sinha A K, Deering C and Briggs C 2010 A model for the origin of rhyolites from South Mountain, Pennsylvania: Implications for rhyolites associated with large igneous provinces; *Lithosphere* **2**(**4**) 211–220, https://doi.org/10.1130/L89.1.

Ross C S and Smith R L 1961 Ash-flow tuffs: Their origin geologic relations and identification; *US Geol. Surv. Prof. Pap.* **360** 81p.

Sarkar S N 1956 Petrography of the rhyolitic conglomerates of east Bhandara, Madhya Pradesh; *Sci. Cult.* **23** 51–53.

Sarkar S N 1957 Stratigraphy and tectonics of Dongargarh system: A new system in the Precambrian of Bhandara–Durg–Balaghat area, Bombay and Madhya Pradesh; *J. Sci. Eng. Res.* **1(2)** 237–268.

Sarkar S N 1958 Stratigraphy and tectonics of Dongargarh system: A new system in the Precambrian of Bhandara–Durg–Balaghat area, Bombay and Madhya Pradesh; *J. Sci. Eng. Res.* **2(2)** 145–160.

Sarkar S N 1994 Chronostratigraphy and tectonics of the Dongargarh supergroup Precambrian rocks in Bhandara–Durg region, central India; *Indian J. Earth Sci.* **21** 19–31.

Sarkar S N, Gopalan K and Trivedi J R 1981 New data on the geochronology of the Precambrians of Bhandara–Durg, central India; *Indian J. Earth. Sci.* **8** 131–151.

Schmid R 1981 Descriptive nomenclature and classification of pyroclastic deposits and fragments: Recommendations of the IUGS Subcommission on the systematics of igneous rocks; *Geology* **9** 41–43.

Sensarma S 2005 The Dongargarh Group: A large Igneous Province at the Archean-Proterozoic Transition in India. *AGU Chapman Conference*, The Great Plume Debate: The origin and impact of LIPs and hot spots **87**.

Sensarma S 2007 A bimodal LIP and the plume debate: The Palaeoproterozoic Dongargarh group, Central India; *Geol. Soc. Am. Spec. Paper* **430** 831–839.

Sensarma S, Hoernes S and Mukhopadhyay D 2004 Relative contributions of crust and mantle to the origin of the Bijli rhyolite in a Palaeoproterozoic bimodal volcanic sequence (Dongargarh group), central India; *J. Earth Syst. Sci.* **113** 619–648, https://doi.org/10.1007/BF02704026.

Sensarma S and Mukhopadhyay D 2003 New insight on the stratigraphy and volcanic history of the Dongargarh belt, central India; *Gondwana Geol. Mag. Spec.* **7** 129–136.

Sensarma S and Mukhopadhyay D 2014 Stratigraphy of the ∼2.5 Ga Dongargarh belt, central India: Key observations and suggested revisions; *Gondwana Geol. Mag. Spec.* **16** 41–48.

Sensarma S and Palme H 2013 Silicate liquid immiscibility in the ∼2.5 Ga Fe-rich andesite at the top of the Dongargarh large igneous province (India); *Lithos* **170–171** 239–251, https://doi.org/10.1016/j.lithos.2013.03.004.

Sensarma S, Palme H and Mukhopadhyay D 2002 Crust-mantle interaction in the genesis of siliceous high magnesian basalts (SHMB): Evidence from the early Proterozoic Dongargarh supergroup, India; *Chem. Geol.* **187** 21–37, https://doi.org/10.1016/S0009-2541(02)00020-7.

Sensarma S, Singh H, Rana R S, Paul D and Sahni A 2017 Nature and composition of interbedded marine basaltic pumice in the ∼52–50 Ma Vastan lignite sequence, western India: Implication for Early Eocene MORB volcanism offshore Arabian Sea; *J. Earth Syst. Sci.* **126**(**2**), https://doi.org/10.1007/s12040-017-0806-2.

Sensarma S, Storey B C and Malviya V P 2018 Gondwana large igneous provinces: Distribution, diversity and significance; *Geol. Soc. London, Spec. Publ.* **463** 1–16.

Sharkove E, Bogina M and Chistyakov A 2017 Magmatic systems of large continental igneous provinces; *Geosci. Frontiers* **8** 621–640, https://doi.org/10.1016/j.gsf.2016.03.006.

Sharma K K 2004 The Neoproterozoic Malani magmatism of the northwestern Indian shield: Implications for crust-building processes; *Proc. Indian Acad. Sci. (Earth Planet. Sci.)* **113(4)** 795–807.

Shellnutt J G, Bhat G M, Wang K-L, Brookfield M E, Dostal J and Jahn B-M 2012 Origin of the silicic volcanic rocks of the Early Permian Panjal traps, Kashmir, India; *Chem. Geol.* **334** 154–170, https://doi.org/10.1016/j.chemgeo.2012.10.022.

Sohn C and Sohn Y K 2019 Distinguishing between primary and secondary volcaniclastic deposits; *Sci. Rep.* **9** 12425, https://doi.org/10.1038/s41598-019-48933-4.

Storm S, Shane P, Schmitt A K and Lindsay J M 2011 Contrasting punctuated zircon growth in two syn-erupted rhyolite magmas from Tarawera volcano: Insights to crystal diversity in magmatic systems; *Earth Planet. Sci. Lett.* **301** 511–520, https://doi.org/10.1016/j.epsl.2010.11.034.

Troll V R, Emeleus C H, Nicoll G R, Mattsson T, Ellam R M, Donaldson C H and Harris C 2019 A large explosive silicic eruption in the British Palaeogene igneous province; *Sci. Rep.*, https://doi.org/10.1038/s41598-018-35855-w.

Vallinayagam G and Kumar N 2007 Volcanic vent in Nakora ring complex of Malani igneous suite, northwestern India; *J. Geol. Soc. India* **70(5)** 881–883.

White J D L, Bryan S E, Ross P-S, Self S and Thordarson T 2009 Physical volcanology of continental large igneous provinces: Update and review. In studies in volcanology: The legacy of George Walker; *IAVCEI Spec. Publ.* **2** 291–321, https://doi.org/10.1144/IAVCEl002.15.

Wilson C J N 2008 Supereruptions and supervolcanoes: Processes and products; *Elements* **4** 29–34, https://doi.org/10.2113/GSELEMENTS.4.1.29.

Wright J V, Smith A L and Self S 1980 A working terminology for pyroclastic deposits; *J. Volcanol. Geotherm. Res.* **8** 315–336, https://doi.org/10.1016/0377-0273(80)90111-0.

Corresponding editor: Jyotisankar Ray